Supplementary Materials

Modelling uncertainty in the relative risk of exposure to the SARS-CoV-2 virus by airborne aerosol transmission in well mixed air in Buildings

Benjamin Jones[a,*], Patrick Sharpe[a], Christopher Iddon[b], E Abigail Hathway[c], Catherine J Noakes[d], Shaun Fitzgerald[e]

[a]*Department of Architecture and Built Environment, University of Nottingham, Nottingham, UK*
[b]*Chartered Institution of Building Services Engineers Natural Ventilation Special Interest Group, 222 Balham High Road, London, UK*
[c]*Department of Civil and Structural Engineering, University of Sheffield, Sheffield, UK*
[d]*School of Civil Engineering, University of Leeds, Leeds, UK*
[e]*Department of Engineering, Cambridge University, Cambridge, UK*

Abstract

This document provides supplementary work to paper given in the title:

B. Jones, P. Sharpe, C. Iddon, E.A. Hathaway, C. Noakes, S. Fitzgerald. Modelling uncertainty in the relative risk of exposure to the SARS-CoV-2 virus by airborne aerosol transmission in well mixed air in Buildings. *Energy & Buildings*. 2021.

*Corresponding author
Email address: benjamin.jones@nottingham.ac.uk (Benjamin Jones)

1. Viral load and viability

The viability of the airborne virions encapsulated in aerosols of respiratory fluid decreases over time through various biological processes. Respiratory fluid is a complex composition of proteins, salts and surfactants and the evaporation of the droplet results in an increase in concentration of these components, which may have an impact on the viability of any encapsulated virions [1]. Biological decay will consider the half-life of the infectivity of the virion containing aerosols which has been measured in the laboratory with median estimates of approximately 1.1 to 1.2 hours and 95% credible intervals of 0.64 to 2.64 for SARS-CoV-2 [2].

2. Aerosol size, breathing rate and viral load of respiratory fluid

Larger droplets produced by expiratory activities, associated with close-proximity direct virus transfer or fomite transmission, or which can become resuspended in air at a later point in time, are not considered in this aerosol airborne transmission model.

The model considers small droplets and droplet nuclei $< 5\,\mu$m that can become entrained in air flows and remain airborne for several hours.

Several studies have measured the range of aerosol sizes emitted during various expiratory activities, although primarily coughs and sneezes, using a range of methodologies [3, 4, 5, 6] and compared by Vuorinen *et al.* [7]. There is a wide variation between individuals taking part in the studies in terms of volumes of aerosols generated through speaking; suggesting a high degree of variability amongst individuals and could in part be related to

the concept of superspreaders, contagious individuals who appear to infect a greater number of secondary individuals, but it is not confirmed.

Recently, the growing availability of higher temporal and spatial visualization methods using high-speed cameras [8], particle image velocimetry [5] and, above all, increasingly accurate particle counters [9] has allowed the detailed characterization and quantification of droplets expelled during various forms of human respiratory exhalation flows (e.g. breathing, whispering, speaking, coughing). This knowledge can be used to estimate the viral load emitted by someone shedding RNA copies into an indoor setting.

Many of the studies on droplet and aerosol expiration have focused on coughs and sneezes. However, as the purpose of this study is to consider asymptomatic and presymptomatic infective individuals, the aerosol generation rate of breathing and talking is of more interest. As most of the aerosols generated by breathing are sub 5 μm, the model uses data produced by Morawska *et al.* which not only measured the volume of sub 5 μm aerosols recorded during breathing but also compared with other expiratory activities that may be conducted by an asymptomatic or pre-symptomatic individual; namely talking and vocalisation (singing an *"aaah"*) which was observed to produce more than 3 and 11 times the number of droplets as produced by mouth breathing, respectively [9]. A 5 μm droplet of pure water evaporates in 0.8 seconds, thus it is assumed that the droplets achieve their equilibrium size before reaching the measurement probe. The aerosols expelled at the mouth could be up to 5 times larger than the measured aerosol, representative of aerosols with an original diameter of up to 27.5 μm and an original volume 125 times greater than the measured aerosol [9, 10].

The number of aerosols are recorded per cm^3 of expired air. To establish a rate of RNA copies emitted by an infector Adams *et al.* will be used as a source of average inhalation rates under various activities [11].

The viral load of respiratory fluid is an important risk factor. A small study recently found the average RNA concentration in sputum of COVID-19 patients to be 7.00×10^6 copies per ml, but with a maximum of 2.35×10^9 copies per ml. During the first week of virus collection 83% of sputum samples were shown to contain viable virus in plaque assays [12]. Miller *et al.* suggest that the RNA concentration could be as high as 1.00×10^{11} copies per ml calculated from RNA copies measured in the air a COVID-19 patient in Singapore [13, 14]. This is a very wide range, of several orders of magnitude.

Using Morawska *et al.* data a total volume of respiratory fluid emitted per cubic metre of exhaled air is calculated. The volume is then used to generate a weighted average droplet diameter which is used in the model, along with the total number of droplets emitted.

Table 1: Number of aerosols in each bin per cm^3 of air in upper respiratory tract.

diameter (μm)	0.800	1.800	3.500	5.500	TOTAL
voiced counting	0.236	0.068	0.007	0.011	0.322
whisper counting	0.110	0.014	0.004	0.002	0.130
vocalisation	0.751	0.139	0.139	0.059	1.088
whisper	0.636	0.037	0.000	0.000	0.673
mouth breathing	0.084	0.009	0.003	0.002	0.098
cough	0.567	0.093	0.012	0.006	0.678

Table 2: Volume (m^3) of respiratory fluid aerosol in each bin per m^3 of exhaled air $\times 10^{-14}$.

Diameter (μm)	0.8	1.8	3.5	5.5	TOTAL
voiced counting	6.33	20.76	15.71	95.83	138.63
whisper counting	2.95	4.28	8.98	17.42	33.63
vocalisation	20.13	42.45	312.05	513.97	888.59
whisper	17.05	11.30	0.00	0.00	28.35
mouth breathing	2.25	2.75	6.73	17.42	29.16
cough	15.20	28.40	26.94	52.27	122.81

Table 3: Weighted average diameter of aerosols for each respiratory activity (μm).

voiced counting	2.02
whisper counting	1.70
vocalisation	2.50
whisper	0.93
mouth breathing	1.78
cough	1.51

Table 4: Viral genomes exhaled assuming a viral load of 3×10^9 RNA copies per ml respiratory fluid of infector and a breathing rate of $0.558\,m^3$ per hour.

Activity	per m^3 exhaled air	per hour	per minute	ratio to breathing
voiced counting	519866	290085	4835	4.75
whisper counting	126099	70363	1173	1.15
vocalisation	3332230	1859385	30990	30.48
whisper	106307	59319	989	0.97
mouth breathing	109341	61012	1017	1.00
cough	460524	256972	4283	4.21

Using Tables 1—4, the generated weighted average diameter of droplets for mouth breathing is 1.78×10^{-6} m. The number of droplets per m^3 of exhaled breath is 98000 ($0.098\,\text{per}\,cm^3$) for breathing.

The volume of fluid in respiratory *aerosols* is 98000 $\times$ the volume of weighted *aerosols*. The sedentary breathing rate for a male [11] is $0.558\,m^3$ per hour.

Assuming an RNA load of 3×10^9 copies per ml (at the high range from Wölfel *et al.* [12]), we multiply this by $5^3 = 125$ on the basis that the measured diameter of the droplets by Morawska *et al.* could be 5 times smaller then the original droplets (i.e. they evaporate on their journey between the mouth and the counting instrument) and therefore the original number of RNA copies in the droplet will be 125 times greater. Stadnytskyi *et al.* [10, 9] give a value of 3.75×10^{17} RNA copies per m^3 of respiratory fluid.

109341 RNA per m^3 exhaled air $\times$ $0.558\,m^3$ per hour = 61012 RNA copies per hour (1017 RNA copies emitted per minute).

This is comparable with Ma *et al.* who estimate between 1000–100,000 RNA copies per minute when breathing (although this is in full range of droplets, so assume 100,000 per minute, 1% of total expired volume in aerosols = 1000 per minute) [15].

In contrast Miller *et al.* assumes 1000-10,000 infectious virions per hour (assume 1 virion per 1000 RNA copies) = 10^6–10^7 RNA copies per hour (16,667—166,667 RNA copies per minute), although this RNA load is representative of a superspreader [13].

3. RNA concentration in respiratory fluid

Breathing and respiratory fluid RNA measurements from COVID-19 patients [12, 15] are used to estimate C_{RNA}. The literature shows a high variability in the concentration of SARS-CoV-2RNA in respiratory secretions ranging from 7.00×10^6 to 1.00×10^{11} RNA copies per ml [10, 12, 13]. In the paper we assume an RNA concentration of 3×10^9 RNA copies per ml, which is equivalent to emitting 16.5 RNA copies per second by breathing. This value is comparable with the lower values of 17 to 1667 RNA copies per second given by Ma *et al.* [15] and the 4.6 RNA copies per second estimated by Miller *et al.* [13] and Chia *et al.* [14] from airborne RNA copies sampled from infected patients in Singapore. We assume that the concentration of RNA copies per ml in respiratory aerosols is 125 times greater to account for evaporation, which reduces the diameter of the exhaled droplets up to five-fold when estimating the total number of RNA copies modelled in aerosols of 5.5 μm and smaller [10]. The size distribution data was measured by Morawska *et al.* to be sufficiently far away from the respiring source to have allowed time for evaporation, thus the measured 5.5 μm diameter aerosols are assumed to have been 27.5 μm at source.

4. Why ventilation flow should be measure in volume per time

The figures in this section highlight why using common ventilation terminology of Air Changes per Hour (h^{-1}) or flow per person per unit time (e.g $1\,l\,s^{-1}$ per person) are not suitable when providing guidance on ventilation rates to minimise the Relative Exposure Index of a space.

4.1. Air changes per hour

If we consider a case with the same attributes as the Reference Scenario classroom, but with $1\,h^{-1}$ and a variable volume, Figure 1 shows that $1\,h^{-1}$ is insufficient in small volume spaces, and over sufficient in very large spaces – because the flow rate per unit time is what drives the ventilation dilution of airborne pollutant.

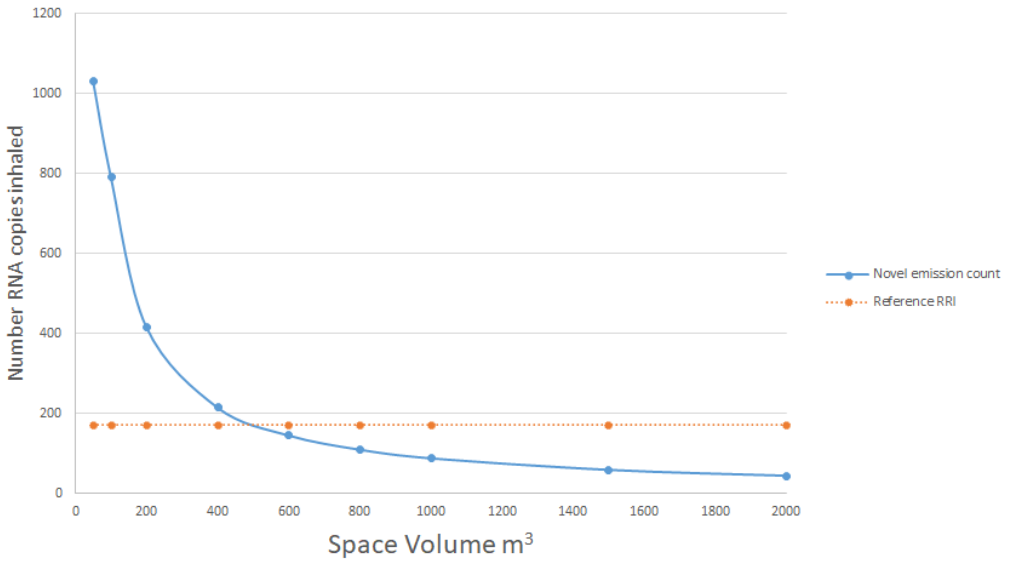

Figure 1: Number of RNA inhaled in spaces, equivalent to the Reference Case, of varying volume with ventilation flow rate of $1\,h^{-1}$.

4.2. Ventilation flow per person per unit time

If we consider a case with the same attributes as the Reference Case classroom, but with varying occupancy and a ventilation flow of $10,1\,s^{-1}$ per person Figure 2 shows that $10\,l\,s^{-1}$ per person is insufficient to reduce the REI when occupancy is low because the total flow rate per unit time is what drives the ventilation dilution of airborne pollutant.

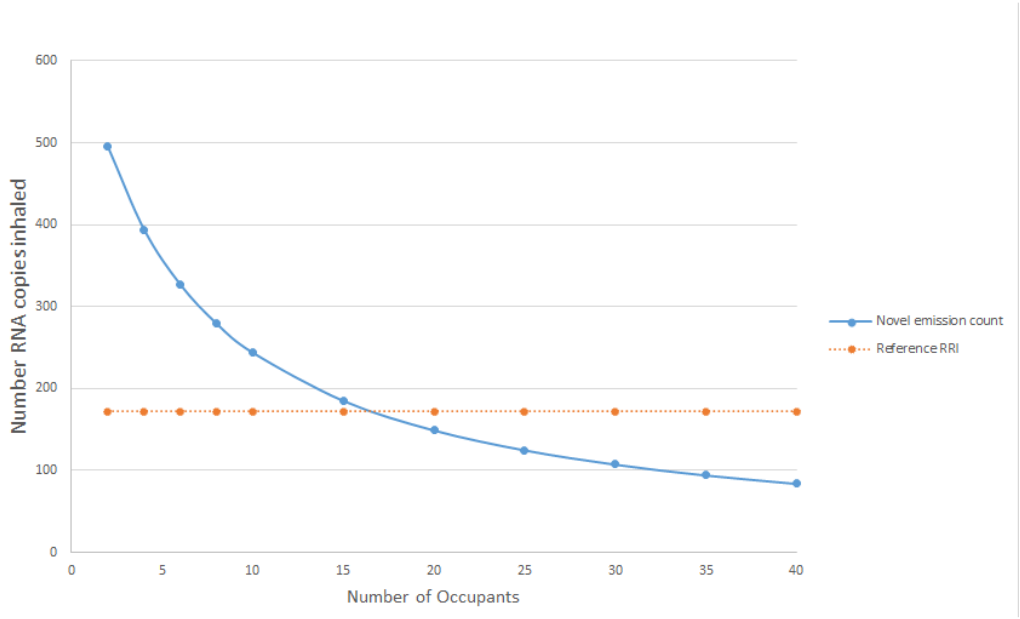

Figure 2: Number of RNA inhaled in Reference Spaces with varying occupancy and a ventilation flow rate of $10\,\mathrm{l\,s^{-1}}$ per person.

In the reference case (discussed in the paper), the flow rate required for an REI = 1.00 a flow rate of $160\,\mathrm{l\,s^{-1}}$ is required.

4.3. Respiratory activities effect on REI

Considering the reference case scenario we consider the index case infector either breathing, talking or vocalisation for the duration of the occupancy period. It is clear that the respiratory activity

Note for vocalisation we have not modelled the increase in breathing rate that would be likely (up to 165% increase suggested by Bernardi *et al.* [16]) so the inhaled RNA copies would be even greater.

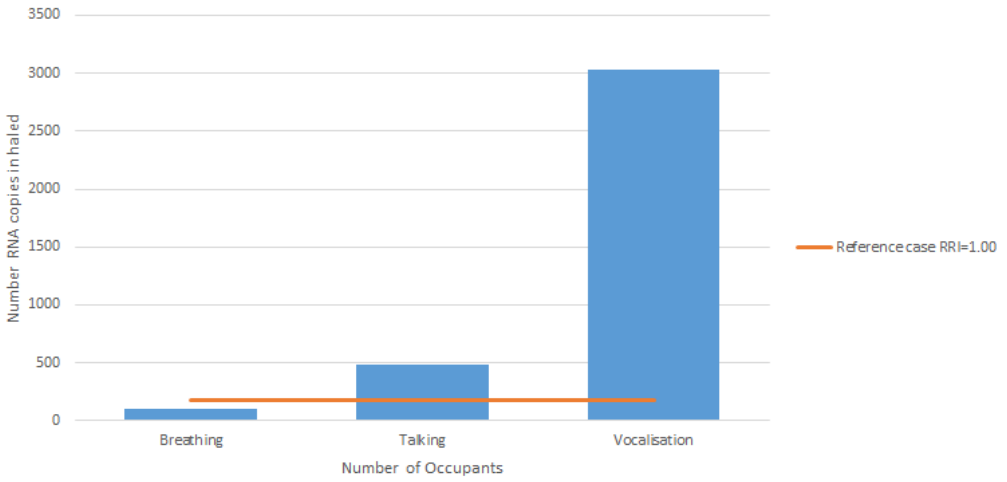

Figure 3: Number of RNA inhaled in Reference Space ventilated at 5l/s/person with the infector undertaking different respiratory activities for the duration of the occupied time.

4.4. Viral load

The viral load in the respiratory fluid of an infector can vary over several orders of magnitude [13, 12]. Figure 4 shows how the inhaled RNA copies is dependent upon the RNA copies load in the respiratory fluid of the infector. The reference case assumes a relatively high load of 3×10^9 RNA copies per ml, however, although the load does not affect the REI, it does affect the inhaled dose of RNA copies and therefore the potential for inhaling infective virions. If the infector RNA load is in the order of 10^6 then in the reference case the inhaled RNA copies is < 1.00 and far field airborne transmission is therefore unlikely. As the RNA load in the respiratory fluid increases, so does the probability of airborne transmission. It is likely that in 1000 RNA copies there may only be 1 viable virion so the probability of infection is exacerbated by the REI [17]. Even with very low REI values it is likely that

144 a superspreader will result in sufficient airborne RNA to be inhaled to lead
145 to infection, but such persons are rare, and therefore using the REI to drive
146 down the risk of an indoor space and activity will result in reducing secondary
147 transmissions, keeping the population $R(t)$ value as low as possible.

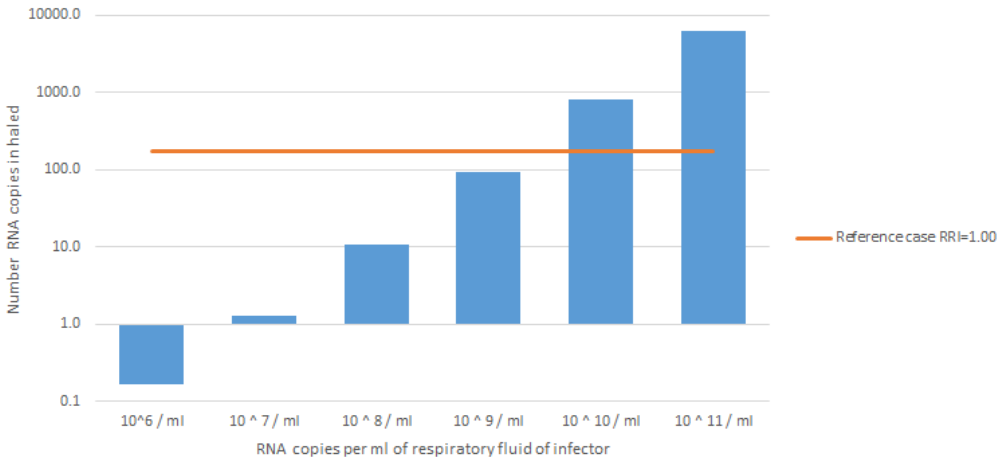

Figure 4: Number of RNA inhaled in Reference Space with varying viral load of infector.

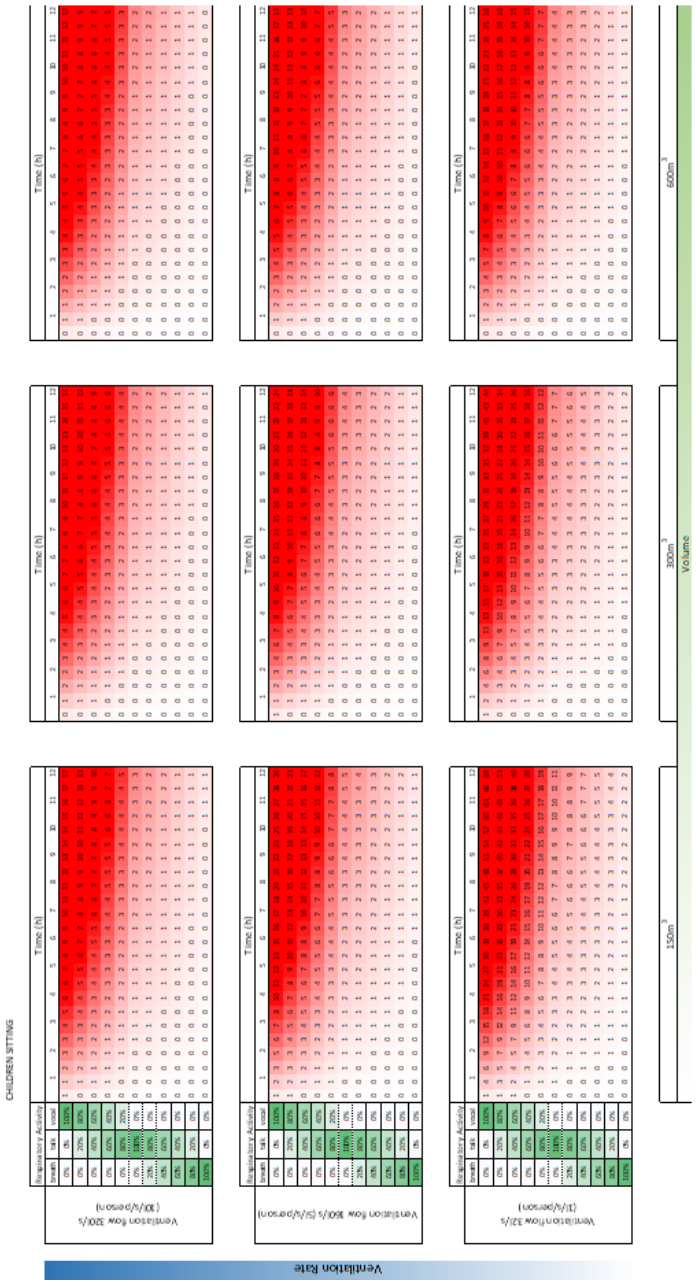

Figure 5: Visualisation of the effect of Occupation Length, Ventilation, Room Volume and Respiratory Activity on REI. Using the breathing rate of Children Sitting, this image demonstrates how the REI changes with respect to increasing the occupation time and with reduced ventilation and smaller room volumes. Values are rounded to nearest whole number.

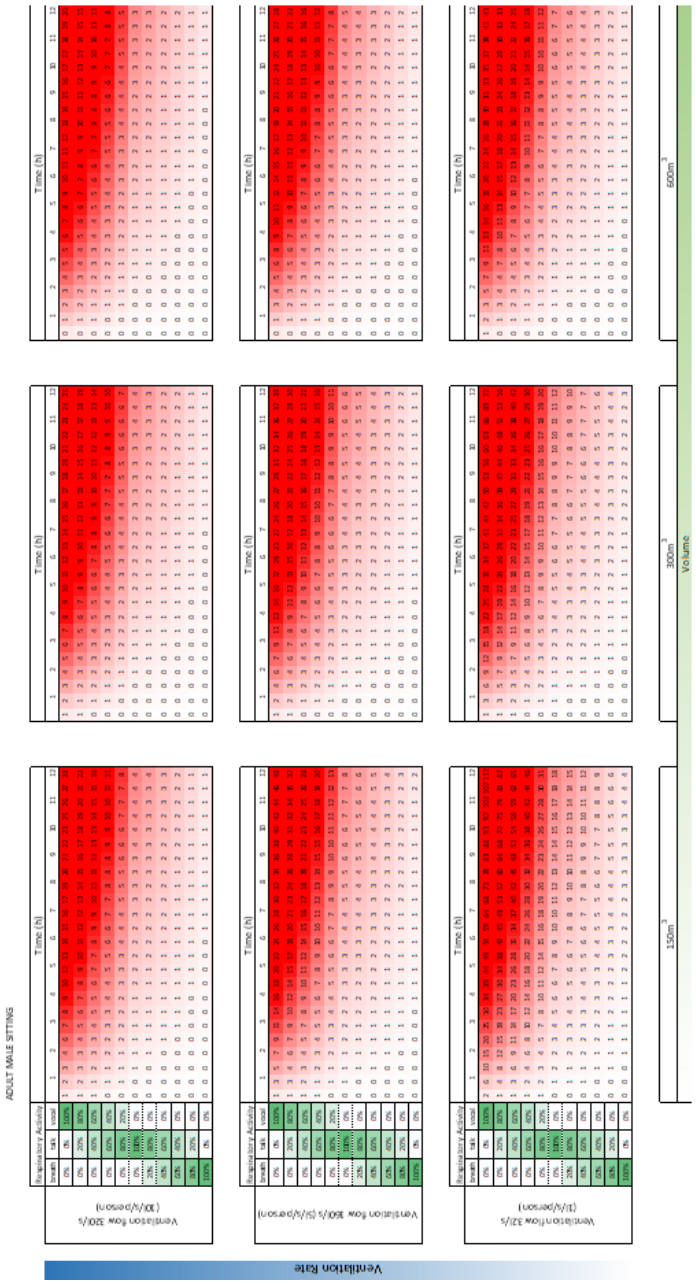

Figure 6: Visualisation of the effect of Occupation Length, Ventilation, Room Volume and Respiratory Activity on REI. Using the breathing rate of Male Sitting, this image demonstrates how the RRI changes with respect to increasing the occupation time and with reduced ventilation and smaller room volumes. Values are rounded to nearest whole number. Note that RRI reference case is a junior classroom with child breathing rates, hence the higher RRI for adult male sitting.

5. Statistical framework

The sampling method follows that described by [18, 19, 20]. The model requires input variates that are either specified deterministically or described by continuous probability distributions to predict $\sum n$.

Deterministic inputs used by all simulations are given in Table 2 in the paper. Five probabilistic inputs apply to all scenarios and their distributions and their governing statistics are given in Table 2 in the main paper. Probabilistic inputs that vary by space type are given in Table 3 in the main paper for each simulated scenario. The values of each probabilistic input using Latin Hypercube Sampling (LHS) to improve the stratification of samples over the probability space [21] and reduces the number of simulations required to reach convergence. They generate a value between 0 and 1 for each input, which are then applied to their inverse cumulative distribution functions (CDF) to generate an input.

Predictions of $\sum n$ are obtained for a set of 1000 samples and a mean $\sum n$ is obtained for each set. After 10 sets (10^5 samples), the means are tested for normality using a one-sample Kolmogorov-Smirnov test, and sampling is stopped when this test is found to be true (p-value $< .01$). Only 10 sets were required to achieve normality in the distribution for all data sets described herein.

For one-off deterministic calculations (see Section 3.1 in the main paper) mean values are used for normally and log-normally distributed variables, and central values are used for uniformly distributed variables.

A sensitivity analysis is used to test the dependence of $\sum n$ on the model

inputs. Here, the method and code[1] [19] of Jones *et al.* is applied and a full description is found in the reference. The method tests for linear (Kendall's τ, Pearson's r, linear regression), monotonic (Spearman's ρ, and rank-transformed standardised variables), and non-monotonic (Kolmogorov–Smirnov and Kruskal–Wallis quantile tests) relationships between inputs and outputs. All inputs are ranked by the magnitude of the regression coefficient. Reported p–values are used to determine variate statistical significant at a 5% level.

A fundamental requirement of a sensitivity analysis is that all tested inputs are independent of one another, and so co-dependent variables should combined. There are no co-depenent variable in this analysis, but there could be in the future. For example, γ_m and G are both a function of droplet diameter but the paucity of data for γ_m means that it is not considered independently of γ.

To quantify the magnitude of the differences between predicted $\sum n$ for the reference space and other spaces, an effect size is used following Ferguson [22] and using Cohen's d. Thresholds are used to label the effects where $d < 0.2$ corresponds to a *negligible* effect size, $0.2 \leq d < 0.5$ to a *small* effect size, $0.5 \leq d < 0.8$ to *medium* effect size, $0.8 \leq d < 1.3$ to a *large* effect size, and $d \geq 1.3$ corresponds to a *very large* effect size.

[1]The code was used under a creative commons license and obtained from DOI: 10.13140/RG.2.2.21670.88644

References

[1] E. P. Vejerano, L. C. Marr, Physico-chemical characteristics of evaporating respiratory fluid droplets, Journal of the Royal Society Interface 15 (139) (2018) 1–10. doi:10.1098/rsif.2017.0939.

[2] N. van Doremalen, T. Bushmaker, D. H. Morris, M. G. Holbrook, A. Gamble, B. N. Williamson, A. Tamin, J. L. Harcourt, N. J. Thornburg, S. I. Gerber, et al., Aerosol and surface stability of sars-cov-2 as compared with sars-cov-1, New England Journal of Medicine 382 (16) (2020) 1564–1567. doi:10.1056/NEJMc2004973.

[3] J. P. Duguid, The Size and the Duration of Air-Carriage of Respiratory Droplets and Droplet-Nuclei, The Journal of Hygiene 44 (6) (1946) 471–9. doi:10.1017/s0022172400019288.

[4] M. Nicas, W. W. Nazaroff, A. Hubbard, Toward understanding the risk of secondary airborne infection: Emission of respirable pathogens, Journal of Occupational and Environmental Hygiene 2 (3) (2005) 143–154. doi:10.1080/15459620590918466.

[5] C. Y. H. Chao, M. P. Wan, L. Morawska, G. R. Johnson, Z. Ristovski, M. Hargreaves, K. Mengersen, S. Corbett, Y. Li, X. Xie, et al., Characterization of expiration air jets and droplet size distributions immediately at the mouth opening, Journal of Aerosol Science 40 (2) (2009) 122–133. doi:10.1016/j.jaerosci.2008.10.003.

[6] X. Xie, Y. Li, H. Sun, L. Liu, Exhaled droplets due to talking and

coughing, Journal of the Royal Society Interface 6 (SUPPL. 6) (2009). doi:10.1098/rsif.2009.0388.focus.

[7] V. Vuorinen, M. Aarnio, M. Alava, V. Alopaeus, N. Atanasova, M. Auvinen, N. Balasubramanian, H. Bordbar, P. Erästö, R. Grande, N. Hayward, A. Hellsten, S. Hostikka, J. Hokkanen, O. Kaario, A. Karvinen, I. Kivistö, M. Korhonen, R. Kosonen, J. Kuusela, S. Lestinen, E. Laurila, H. Nieminen, P. Peltonen, J. Pokki, A. Puisto, P. Råback, H. Salmenjoki, T. Sironen, M. Österberg, Modelling aerosol transport and virus exposure with numerical simulations in relation to SARS-CoV-2 transmission by inhalation indoors, Safety Science 130 (May) (2020) 104866. arXiv:2005.12612, doi:10.1016/j.ssci.2020.104866.
URL http://arxiv.org/abs/2005.12612

[8] J. W. Tang, C. J. Noakes, P. V. Nielsen, I. Eames, A. Nicolle, Y. Li, G. S. Settles, Observing and quantifying airflows in the infection control of aerosol- and airborne-transmitted diseases: An overview of approaches, Journal of Hospital Infection 77 (3) (2011) 213–222. doi:10.1016/j.jhin.2010.09.037.

[9] L. Morawska, G. R. Johnson, Z. D. Ristovski, M. Hargreaves, K. Mengersen, S. Corbett, C. Y. Chao, Y. Li, D. Katoshevski, Size distribution and sites of origin of droplets expelled from the human respiratory tract during expiratory activities, Journal of Aerosol Science 40 (3) (2009) 256–269. doi:10.1016/j.jaerosci.2008.11.002.

[10] V. Stadnytskyi, C. E. Bax, A. Bax, P. Anfinrud, The airborne lifetime of small speech droplets and their potential importance in SARS-CoV-2

transmission., Proceedings of the National Academy of Sciences of the United States of America (2020) 3–5doi:10.1073/pnas.2006874117.
URL http://www.ncbi.nlm.nih.gov/pubmed/32404416

[11] A. WC, Measurement of breathing rate and volume in routinely performed daily activities, Final report, contract no. a033-205., California Air Resources Board, Sacramento (1996).

[12] R. Wölfel, V. M. Corman, W. Guggemos, M. Seilmaier, S. Zange, M. A. Müller, D. Niemeyer, T. C. Jones, P. Vollmar, C. Rothe, M. Hoelscher, T. Bleicker, S. Brünink, J. Schneider, R. Ehmann, K. Zwirglmaier, C. Drosten, C. Wendtner, Virological assessment of hospitalized patients with COVID-2019, Nature 581 (March) (2020). doi:10.1038/s41586-020-2196-x.
URL http://dx.doi.org/10.1038/s41586-020-2196-x

[13] S. L. Miller, W. W. Nazaroff, J. L. Jimenez, A. Boerstra, S. J. Dancer, J. Kurnitski, L. C. Marr, L. Morawska, C. Noakes, Transmission of SARS-CoV-2 by inhalation of respiratory aerosol in the Skagit Valley Chorale superspreading event, MedRxiv preprint preprint (June) (2020) 1–17. doi:https://doi.org/10.1101/2020.06.15.20132027.

[14] P. Y. Chia, K. K. Coleman, Y. K. Tan, S. Wei, X. Ong, M. Gum, S. K. Lau, X. F. Lim, A. S. Lim, S. Sutjipto, P. H. Lee, T. T. Son, B. E. Young, D. K. Milton, G. C. Gray, S. Schuster, T. Barkham, P. P. De, S. Vasoo, M. Chan, B. Sze, P. Ang, Detection of air and surface contamination by SARS-CoV-2 in hospital rooms of infected patients, ? (2020). doi:10.1038/s41467-020-16670-2.

[15] J. Ma, X. Qi, H. Chen, X. Li, Z. Zhang, H. Wang, L. Sun, L. Zhang, J. Guo, L. Morawska, S. A. Grinshpun, P. Biswas, R. C. Flagan, M. Yao, Covid-19 patients in earlier stages exhaled millions of sars-cov-2 per hour, Clinical Infectious Diseases-Ciaa1283 (08 2020). arXiv:https://academic.oup.com/cid/advance-article-pdf/doi/10.1093/cid/ciaa1283/33693557/ciaa1283.pdf, doi:10.1093/cid/ciaa1283.
URL https://doi.org/10.1093/cid/ciaa1283

[16] N. F. Bernardi, S. Snow, I. Peretz, H. D. Orozco Perez, N. Sabet-Kassouf, A. Lehmann, Cardiorespiratory optimization during improvised singing and toning, Scientific Reports 7 (1) (2017) 1–8. doi:10.1038/s41598-017-07171-2.
URL http://dx.doi.org/10.1038/s41598-017-07171-2

[17] J. Yan, M. Grantham, J. Pantelic, P. J. B. De Mesquita, B. Albert, F. Liu, S. Ehrman, D. K. Milton, Infectious virus in exhaled breath of symptomatic seasonal influenza cases from a college community, Proceedings of the National Academy of Sciences of the United States of America 115 (5) (2018) 1081–1086. doi:10.1073/pnas.1716561115.

[18] P. Das, C. Shrubsole, B. Jones, I. Hamilton, Z. Chalabi, M. Davies, A. Mavrogianni, J. Taylor, Using probabilistic sampling-based sensitivity analyses for indoor air quality modelling, Building and Environment 78 (2014) 171–182.

[19] B. Jones, P. Das, Z. Chalabi, M. Davies, I. Hamilton, R. Lowe, A. Mavrogianni, D. Robinson, J. Taylor, Assessing uncertainty in housing stock

infiltration rates and associated heat loss: English and UK case studies, Building and Environment 92 (2015) 644–656.

[20] C. O'Leary, B. Jones, S. Dimitroulopoulou, I. Hall, Setting the standard: The acceptability of kitchen ventilation for the english housing stock, Building and Environment (2019) In- doi:https://doi.org/10.1016/j.buildenv.2019.106417.
URL http://www.sciencedirect.com/science/article/pii/S0360132319306274

[21] J. C. Helton, F. J. Davis, Latin hypercube sampling and the propagation of uncertainty in analyses of complex systems, Reliability Engineering & System Safety 81 (1) (2003) 23–69.

[22] C. J. Ferguson, An effect size primer: A guide for clinicians and researchers, Professional Psychology: Research and Practice 40 (5) (2009) 532.